Octagonal Quasi-Photonic Crystal Single-Defect Microcavity With Whispering Gallery Mode and Condensed Device Size

Po-Tsung Lee, *Member, IEEE*, Tsan-Wen Lu, and Feng-Mao Tsai

***Abstract*—We propose a new single-defect microcavity which supports well-confined whispering gallery mode in octagonal quasi-photonic crystals (OQPC) by shifting the eight nearest air holes around the cavity. Lasing action is observed and compared with the calculated results obtained using the finite-difference time-domain method. We also investigate the threshold dependence on the number of lattice periods of this OQPC microcavity and compare it with triangular lattice photonic crystal (PC) microcavity with similar cavity size. The OQPC microcavity exhibits only a 36% increase of threshold when the number of lattice periods decreases from eight to four, which is more advantageous than the triangular lattice PC microcavity for the shrinkage of device size.**

***Index Terms*—Microcavity, quasi-photonic crystal (QPC), semiconductor lasers.**

PHOTONIC crystal (PC), a kind of artificial lattice structure, has attracted much attention due to the possibilities and abilities of controlling the flow of photons in recent years. The electromagnetic wave propagation inside a PC is forbidden for some specific or all directions for a certain frequency range due to the photonic bandgap (PBG) effect [1]. However, it has been reported that there is anisotropy of PBG in PC caused by the low-level rotational symmetry in its Brillouin zone [2], [3]. Higher rotational symmetry leads to more circular Brillouin zone and less anisotropy of PBG. In order to reach this target, the concept of quasi-crystal in solid-state physics is applied. In very recent years, the existence of large and isotropic PBGs in different quasi-photonic crystals (QPCs) has been reported [4]–[7]. In general, QPCs can be classified into penrose (five-fold), octagonal (eight-fold), decagonal (ten-fold), dodecagonal (12-fold), and so on according to their rotational symmetries. QPCs, which served as the mirror of microcavities, have been investigated in theory by several groups [8]–[10]. Although few experimental results for dodecagonal QPCs (DQPCs) have been reported [9], [10], there are no experimental results for other QPCs. In this report, we propose a new cavity design using OQPC with well-confined whispering gallery mode (WGM) based on finite-difference time-domain (FDTD) simulations. We fabricate the device and obtain single-mode lasing action. The threshold dependence on different lattice periods surrounding the microcavity is also investigated.

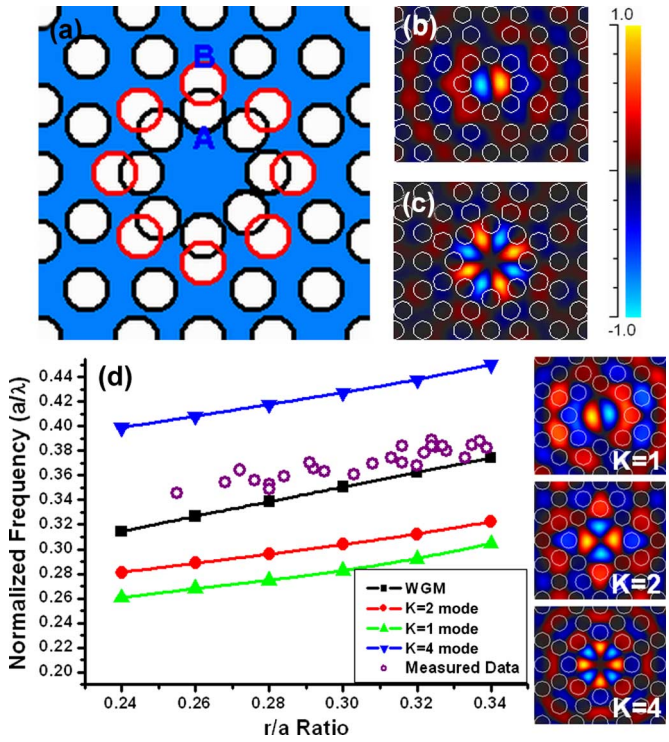

Fig. 1. (a) Schematic of original (position A) and modified (position B) OQPC single-defect microcavity. (b) Calculated dipole mode and (c) calculated WGM profiles of these two microcavities. (d) Defect modes in normalized frequency of modified single-defect OQPC microcavity as a function of r/a ratio. The circles denote the measured data, which match with WGM.

The lasing action of a DQPC microcavity is demonstrated by Nozaki *et al.* [9]. The geometry of DQPC microcavity is similar with that of the microgear laser [11] and the gears formed at the cavity edge have good consistency with the WGM [12]. Thus, lasing action is affected not only by the PBG effect but also by the total-internal-reflection effect. Under this fusion, WGM with a high-quality (Q)-factor can still be sustained when the cavity size is reduced to the diffraction-limited size in microdisk lasers. The similar concept used to enhance high-Q WGM in PC microcavity is also investigated by Ryu *et al.* [13]. Here we propose that the similar fusion and smaller cavity size with high-Q WGM can be achieved in OQPC single-defect microcavity by proper modifications. The schematic of OQPC single-defect microcavity is shown in Fig. 1(a). At first, we

Manuscript received April 17, 2006; revised October 4, 2006. This work was supported by Taiwan's National Science Council under Contract NSC-95-2221-E-009-234 and Contract NSC-95-2221-E-009-056, and by Promoting Academic Excellence of Universities under Contract NSC-94-2752-E-009-007-PAE.

The authors are with the Department of Photonics and Institute of Electro-Optical Engineering, National Chiao Tung University, Hsinchu 300, Taiwan, R.O.C. (e-mail: ricky.eo94g@nctu.edu.tw).

Color versions of one or more of the figures in this letter are available online at http://ieeexplore.ieee.org.

Digital Object Identifier 10.1109/LPT.2007.895054

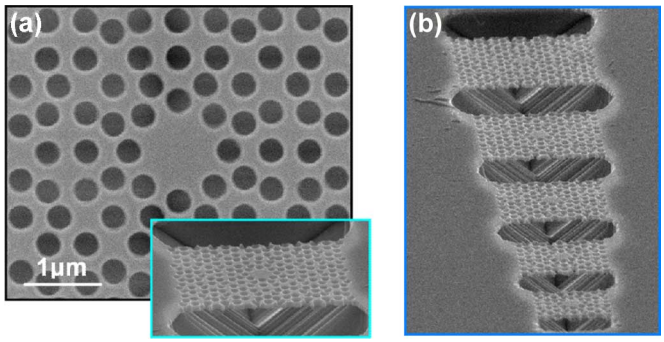

Fig. 2. (a) Top-view SEM picture of a typical modified OQPC single-defect microcavity. The inset shows its titled-view image. (b) Titled-view SEM image of modified OQPC single-defect microcavities with lattice periods eight to four from top to bottom.

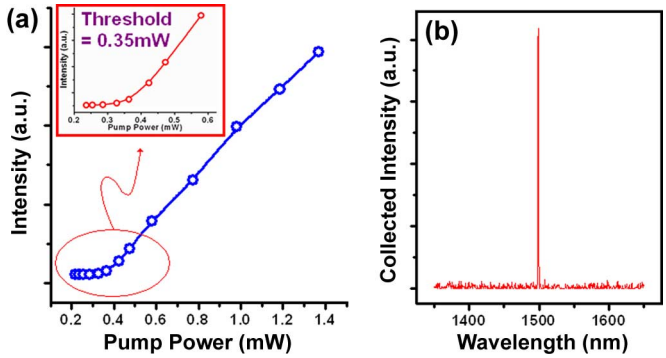

Fig. 3. (a) L–L curve. The inset shows the L–L curve near threshold and indicates its threshold as low as 0.35 mW. (b) Lasing spectrum at 1499 nm with 0.15-nm FWHM.

calculate its defect mode using the two-dimensional (2-D) FDTD method with effective index 2.7 of the dielectric material. The approximated simulation method used here is a quite efficient and reliable approach. We compare its precision with three-dimensional (3-D) FDTD simulation using typical PC single-defect microcavity. There are only about 3% $\sim$ 5% wavelength red shifts in 2-D FDTD simulations and no significant difference observed in mode profile calculations. The designed air hole radius (r) over lattice constant (a) is 0.3. The typical dipole mode profile in the magnetic field is obtained as shown in Fig. 1(b). In order to obtain the well-confined WGM, the eight nearest air holes are shifted outward from position A to position B, as shown in Fig. 1(a), until the distance between two neighboring air holes is equal to the lattice constant in order to satisfy the constructive interference condition for the standing wave at the cavity boundary. The epitaxial wafer is grown by plasma-enhanced chemical vapor deposition system. And the polymerthylmethacrylate (PMMA) layer is spin-coated on the SiN_x layer. The OQPC patterns are defined on the PMMA layer by electron-beam (e-beam) lithography and transferred to the SiN_x layer by the reactive-ion etching process with CHF_3–O_2 mixed gas. Then the patterns are further transferred to multiquantum wells (MQWs) by inductively coupled plasma dry-etching with CH_4–Cl_2–H_2 mixed gas at 150 °C. At last, the membrane structure is formed by selective wet etching with the mixture of HCl and H_2O at 0 °C. The top-view and tilted-view scanning electron microscope (SEM) picture of the device is shown in Fig. 2(a) and its inset. The fabricated r/a ratio is 0.294 with 550-nm lattice constant. The cavity size is about 1.2 μm in diameter, which is smaller than the diffraction-limited size of microdisk lasers.

In characterization, the microcavity is pumped by an 845-nm laser diode with 0.5% duty cycle and 0.2-MHz repetition rate in order to avoid the thermal problems. The emitted light is collected by an optical spectrum analyzer with 0.05-nm spectrum resolution. The light-in light-out curve (L–L curve) and the typical lasing spectrum of the fabricated microcavity laser with r/a ratio 0.32 and lattice constant 550 nm at room temperature are shown in Fig. 3(a) and (b). Its threshold is as low as 0.35 mW and the effective threshold incident pump power is estimated to be smaller than 90 μW. The central lasing wavelength is 1499 nm with full-width at half-maximum (FWHM) 0.15 nm and a high sidemode suppression ratio (SMSR) larger than 25 dB is observed. The SMSR can be improved to 30 $\sim$ 35 dB by inserting an air hole in the central of the cavity region without disturbing the WGM. The details of experimental results and discussion are published elsewhere [14]. Its Q-factor is about 7500, which is estimated from the measured linewidth (Δ_{FWHM}) at the transparency pump level by $Q = \lambda/\Delta_{\mathrm{FWHM}}$. This experimental estimated method is also used in reports by other groups [15], [16]. This high-Q value can be attributed to the well-confined characteristics of WGM with standing wave formed in the gears around the edge of cavity. In order to identify the lasing mode, we fabricate various devices with different r/a ratios from 0.25 to 0.34 and different lattice constants from 530 to 570 nm. The measured lasing wavelengths denoted by open circles in Fig. 1(d) quite agree with the simulated results and we can identify the lasing mode as WGM. Furthermore, observation of lasing action with an added central air hole mentioned above also provides further evidence that the lasing mode is WGM. The small difference in normalized frequency between the calculated and experiment results is caused by the 2-D effective index approximation we discussed before and the unavoidable dimension estimation inaccuracy from SEM pictures.

We also fabricate modified OQPC single-defect microcavity arrays with different lattice periods from eight to three. The tilted-view SEM picture is shown in Fig. 2(b). The plot of lasing threshold versus number of cladding lattice periods is shown in Fig. 4. The threshold of OQPC microcavity with eight lattice periods is 0.71 mW and the lasing wavelength is 1454 nm. The higher threshold of this cavity than the one in Fig. 3 is caused by different gain spectrum alignment. In Fig. 4, the thresholds are almost the same when the number of lattice periods is larger than six. Although the threshold increases when the number of lattice periods is smaller than six, the threshold with four lattice periods is 0.95 mW, which is only 36% increase compared to that with eight lattice periods. With four cladding lattice periods, the device size is only 3.5 μm $\times$ 3.5 μm, as shown in the inset SEM picture of Fig. 4, which is a very condensed device size ever reported. Lasing action is not always observed when the number of lattice periods is reduced to three. We also fabricate triangular lattice PC microcavity with similar cavity size formed by seven missing air holes (D2 cavity) for comparison. The fabricated r/a ratio and lattice constant are 0.29 and 480 nm. As shown in Fig. 4, the thresholds of triangular

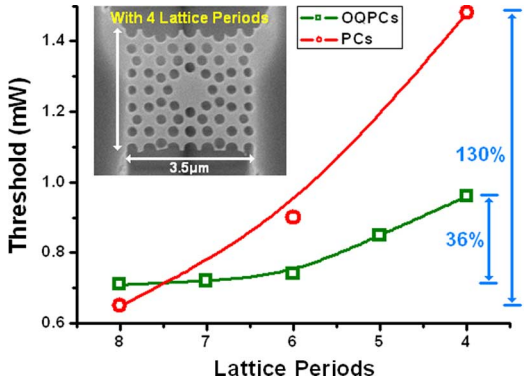

Fig. 4. Plot of lasing threshold versus number of cladding lattice periods. There is only 36% increase in threshold of OQPC microcavity when the number of lattice periods is reduced from eight to four, which is much smaller than the 130% of triangular lattice PC D2 microcavity. The inset shows the SEM image of the OQPC microcavity with four lattice periods and very condensed size of $3.5\ \mu\text{m} \times 3.5\ \mu\text{m}$.

lattice PC D2 microcavities with eight, six, and four cladding lattice periods are 0.65, 0.9, and 1.48 mW, respectively. And the lasing wavelength is near 1560 nm, which aligns better with the gain peak of MQWs, leading to a smaller threshold of triangular lattice PC D2 microcavity with eight lattice periods than that of OQPC microcavity. For the number of lattice periods below seven, one can see that the thresholds of OQPC microcavities are much lower than that of triangular lattice PC D2 microcavity even the lasing wavelength of the former is much farther away from the gain peak of MQWs. In addition, the threshold of triangular lattice PC D2 microcavity increases about 130% from eight periods to four periods, which is much larger than the 36% of OQPC microcavities. In triangular lattice PC D2 microcavity, the lasing mode is similar to A1 mode [17] instead of WGM, which is due to the low-Q factor (only several hundred or lower) of WGM in it [13]. However, a high-Q WGM can be sustained in OQPC single-defect microcavity, and its performance is even better than the high-Q mode in triangular lattice PC D2 microcavity.

From the simulated and measured results, we demonstrate the existence of high-Q WGM in a modified OQPC single-defect microcavity. The significant zero field distribution central node of WGM is very suitable for the design of current-injection structure with a central post under the cavity region without disturbing the lasing mode. Besides, this device shows better lasing characteristics and smaller threshold degradation with condensed device size compared to PC lasers, which is ascribed to the more uniform and efficient confinement provided by the OQPC lattice. As a result, this device can be placed in a localized region in an integrated photonic system and its lasing characteristics will not be affected significantly when the parameters of the neighboring devices are changed. In addition, this also confirms that one can fuse only a few lattice periods of OQPC at the disk edge of microdisk laser to provide efficient confinement and achieve high-Q WGM lasing below the diffraction-limited microdisk size.

In summary, we have designed a modified OQPC single-defect microcavity which supports a well-confined WGM based on 2-D FDTD simulations and the measured results from the fabricated devices show a clear correspondence. Ultralow threshold as low as 0.35 mW and estimated high-Q factor 7500 are obtained. We also investigated the threshold dependence on different cladding lattice periods. Lasing action of a very condensed-size device ($3.5\ \mu\text{m} \times 3.5\ \mu\text{m}$) is still observed when the number of lattice periods is reduced to four, which is a potentially active device in future integrated photonic circuit and communication system applications. Its threshold degradation 36% is much smaller than 130% of the triangular lattice PC microcavity with a similar cavity size.

ACKNOWLEDGMENT

The authors would like to thank T.-C. Lu, H.-C. Kuo, and the Center for Nano Science and Technology in National Chiao Tung University, Taiwan, R.O.C., for their help.

REFERENCES

[1] E. Yablonovitch, "Inhibited spontaneous emission in solid-state physics and electronics," *Phys. Rev. Lett.*, vol. 58, pp. 2059–2062, 1987.
[2] D. Cassagne, C. Jouanin, and D. Bertho, "Hexagonal photonic-band-gap structures," *Phys. Rev. B*, vol. 53, pp. 7134–7142, 1996.
[3] A. Barra, D. Cassagne, and C. Jouanin, "Existence of two-dimensional absolute photonic band gaps in the visible," *Appl. Phys. Lett.*, vol. 72, pp. 627–629, 1998.
[4] Y. S. Chan, C. T. Chan, and Z. Y. Liu, "Photonic band-gaps in two-dimensional photonic quasi-crystals," *Phys. Rev. Lett.*, vol. 80, pp. 956–959, 1998.
[5] M. E. Zoorob, M. D. B. Charlton, G. J. Parker, J. J. Baumberg, and M. C. Nett, "Complete photonic band-gaps in 12-fold symmetric quasi-crystals," *Nature (London)*, vol. 404, pp. 740–743, 2000.
[6] C. J. Jin, B. Y. Cheng, B. Y. Man, Z. L. Li, and D. Z. Zhang, "Two-dimensional dodecagonal and decagonal quasi-periodic photonic crystals in the microwave region," *Phys. Rev. B*, vol. 61, pp. 762–767, 2000.
[7] M. Bayindir, E. Cubukcu, I. Bubu, and E. Ozbay, "Photonic bandgap effect, localization, and waveguiding in the two-dimensional Penrose lattice," *Phys. Rev. B.*, vol. 63, p. 161104, 2001.
[8] J. Chaloupka, J. Zarbakhsh, and K. Hingerl, "Local density of states and modes of circular photonic crystal cavityies," *Phys. Rev. B*, vol. 72, p. 085122, 2005.
[9] K. Nozaki and T. Baba, "Quasi-periodic photonic crystal micro-cavity lasers," *Appl. Phys. Lett.*, vol. 84, pp. 4875–4877, 2004.
[10] S. K. Kim, J. H. Lee, S. H. Kim, I. K. Hwang, Y. H. Lee, and S. B. Kim, "Photonic quasi-crystal single-cell cavity mode," *Appl. Phys. Lett.*, vol. 86, p. 031101, 2005.
[11] M. Fujita and T. Baba, "Microgear laser," *Appl. Phys. Lett.*, vol. 80, pp. 2051–2053, 2002.
[12] K. Nozaki, A. Nakagawa, D. Sano, and T. Baba, "Ultralow threshold and single-mode lasing in microgear lasers and its fusion with quasi-periodic photonic crystals," *IEEE J. Sel. Top. Quantum Electron.*, vol. 9, no. 5, pp. 1355–1360, Sep./Oct. 2003.
[13] H. Y. Ryu, M. Notomi, G. H. Kim, and Y. H. Lee, "High quality-factor whispering-gallery mode in the photonic crystal hexagonal disk cavity," *Opt. Express*, vol. 12, pp. 1708–1719, 2004.
[14] P. T. Lee, T. W. Lu, F. M. Tsai, T. C. Lu, and H. C. Kuo, "Whispering-gallery-mode of modified octagonal quasi-periodic photonic crystal single-defect micro-cavity and its side-mode reduction," *Appl. Phys. Lett.*, vol. 88, p. 201104, 2006.
[15] K. Srinivasan, P. E. Barclay, O. Painter, J. Chen, A. Y. Cho, and C. Gmachl, "Experimental demonstration of a high quality factor photonic crystal microcavity," *Appl. Phys. Lett.*, vol. 83, pp. 1915–1917, 2003.
[16] H. G. Park, S. H. Kim, M. K. Seo, Y. G. Ju, S. B. Kim, and Y. H. Lee, "Characteristics of electrically driven two-dimensional photonic crystal lasers," *IEEE J. Quantum Electron.*, vol. 41, no. 9, pp. 1131–1141, Sep. 2005.
[17] W. Kuang, J. R. Cao, S. J. Choi, P. T. Lee, J. D. O'Brien, and P. D. Dapkus, "Classification of modes in suspended membrane, 19 missing hole photonic-crystal micro-cavities," *J. Opt. Soc. Amer. B*, vol. 83, pp. 4107–4109, 2005.